Lawrence Berkeley National Laboratory
Recent Work

Title
THE MARTENSITE PHASES IN 304 STAINLESS STEEL

Permalink
https://escholarship.org/uc/item/13d8k8jq

Authors
Mangonon, P.L.
Thomas, G.

Publication Date
1969-06-01

THE MARTENSITE PHASES IN 304 STAINLESS STEEL

P. L. Mangonon, Jr. and G. Thomas

June 1969

LAWRENCE RADIATION LABORATORY
UNIVERSITY of CALIFORNIA BERKELEY

DISCLAIMER

THE MARTENSITE PHASES IN 304 STAINLESS STEEL

by

P. L. Mangonon[+] and G. Thomas

Inorganic Materials Research Division, Lawrence Radiation Laboratory,
Department of Materials Science and Engineering, College of Engineering,
University of California, Berkeley, California

ABSTRACT

A detailed analysis of martensite transformations in 18/8 (304) stain-
less steel, utilizing transmission electron microscopy and diffraction in
conjunction with X-ray and magnetization techniques, has established that
the sequence of transformation is $\gamma \to \varepsilon \to \alpha$. ε is a thermodynamically
stable hcp phase whose formation is greatly enhanced as a result of plastic
deformation. Comparison with the $\varepsilon \to \alpha$ transformation in pure Fe-Mn alloys
lends further support to the above sequence and suggests that a transforma-
tion line between ε and α in Fe-Cr-Ni alloys can be expected. In the 304
stainless steel used in this investigation, formation of α was induced only
by plastic deformation and subsequent to formation of ε. Nucleation of α
occurs heterogeneously at intersections of ε-bands or where ε-bands abutt
twin or grain boundaries (which represent unilaterally compressed regions).
From electron diffraction, the Nishiyama relationship between γ and α
phases appears to predominate at the start of the transformation, but then
changes to that of Kurdjumov-Sachs. Based on these observations, a sequence
of atom movements from the hcp structure to the bcc structure is proposed
which has the basic geometric features of the martensitic transformation.

+Present address: Inland Steel Co. Research Laboratories
East Chicago, Indiana 46312

I. INTRODUCTION

The martensitic transformation from the fcc to the bcc phase in 18/8 type austenitic stainless steels is complicated by the presence of the hcp (ε) phase which is always found to be closely associated with the α. Both the transformation products, ε and α, are believed to transform martensitically in that a shape change was observed in each case, although, as pointed out by Wayman[1] in a very recent review, the shape change has not yet been verified to conform to an invariant plane strain. It is possible for these phases to be obtained either by direct quenching of the austenite or by stress-inducing the transformations, although it is not clear whether in 18/8 that α can be produced just by quenching.

The structural characteristics of the ε and α phases in these alloys have been widely investigated using both optical[2-7] and transmission electron microscopy[7-13] in conjunction with X-ray techniques. The presence of the strong $(10\bar{1}0)_\varepsilon$[8] reflection and also the double diffraction spot $(0001)_\varepsilon$[8] in electron diffraction patterns implied that ε was hexagonal rather than fcc containing a high density of randomly distributed faults. The ε phase has been observed to occur as dark bands on $\{111\}_\gamma$ planes with the α forming within the width of these bands. Kelly[13] describes α as lath-like, which differs from the needle-like[12] and plate-like[4] descriptions of previous investigators. It appears also that the orientation relationship between the γ and α phases corresponds to the Kurdjumov-Sachs relationship, although the crystallography and mode of the α martensite formation differs from that in the Fe-C, Fe-Ni-C and Fe-Ni alloys.[1,10,13]

The close association of α and ε in these alloys gives rise to the natural question as to which phase forms first. Two possibilities arise:

1) ϵ forms first and α nucleates within ϵ or, 2) the austenite transforms directly to α with the ϵ being formed as a consequence of the rather large shape deformation ($\sim 10°$) of the $\gamma \rightarrow \alpha$ transformation and the low stacking fault energy of the untransformed austenite. In spite of the numerous investigations devoted to this question, no unambiguous resolution has yet been attained.[1] Cina[2,3] found the amount of ϵ became a maximum and later decreased in quantity while the amount of α progressively increased. This observation led him to believe that α nucleated from ϵ. Reed[4] showed by stain-etching that long α-plates were induced alongside bands of ϵ after repeated cyling from room temperature to sub-zero temperatures. Venables[8] and Lagneborg,[7] using transmission electron microscopy, showed that the α was preferentially nucleated at intersections of two ϵ-bands or an ϵ-band and an active slip plane. On the other hand, Otte and Dash[9,10] and Breedis[11] took the second point of view that ϵ forms only because of the large shape deformation due to the $\gamma \rightarrow \alpha$ transformation. It has been further argued[9] from symmetry considerations that the transformation from a structure of lower symmetry (i.e., hcp) to one of higher symmetry (i.e., bcc) is highly unlikely. Furthermore, Goldman, Robertson and Koss[14] argued that a different M_s temperature should be observed for the $\gamma \rightarrow \epsilon$ transformation, from that due to the $\gamma \rightarrow \alpha$ or $\epsilon \rightarrow \alpha$ transformations. Since a difference was not found, the ϵ was concluded not to be an intermediate phase. Wayman[1] has argued from the theoretical calculations of Kelly[13] that the inhomogeneous shear ($m_2 = 0.35$) is too large to permit classification to a lattice invariant shear and the overall transformation to be of the fcc$\rightarrow$bcc type. In this respect, Wayman[1] supports the view that ϵ forms as a consequence of the α formation. With the latter point of view, ϵ should be expected to increase proportionately with increasing amounts of α, and also that ϵ should never be observed unless

α is already present. However, Cina,[3] Guntner and Reed[15] showed that this

cannot be the case since ε decreased in amount after attaining a certain maxi-

mum quantity. Otte and Dash[9] suggested that unfaulting occurred by re-

combination of partial dislocations before γ transformed to α. This might

very well explain the decrease in amount of ε phase, and implies very strongly

that the ε phase cannot be contained within the bounds of the α-phase.

The present investigation was undertaken to clarify the actual sequence

of events in the transformation, and to learn more of the nucleation mechanisms.

A further investigation of the changes in mechanical properties resulting

from thermal - mechanical treatments to produce α is described in a second

paper.[17]

II. EXPERIMENTAL TECHNIQUES

The composition of the alloy was 18.03% Cr, 8.46% Ni, 1.32% Mn, 0.07% C, 0.72% Si, 0.015% P, 0.006% S, 0.08% Co and the balance Fe.

Tensile specimens with gage section 2-1/4"x 1/2" were obtained from the 0.030-inch thick 304 stainless steel sheet stock. All specimens were annealed at 1100°C for 30 minutes in argon atmosphere and then quenched in water. Some specimens were quenched directly to liquid nitrogen (78°K) and helium (4°K) and one specimen into dry ice-acetone bath (∿195°K) and held for 3 days. Sensitive magnetic measurements[16] showed that α did not form after these treatments, and indicate that the M_s for α must be below 4°K. In order to induce formation of α, the specimens were deformed in an Instron machine up to a uniform tensile elongation of 24% and 40% (in 2"-gage length) at liquid nitrogen and room temperatures, respectively. α was detected after a tensile strain of only 0.25% at LN temperature, whereas no evidence for α was observed up to 40% strain at room temperature. Rolling deformation at 78°K was also done up to 20% reduction in thickness. The material was intermittently dipped in liquid nitrogen between 0.001" maximum rolling reductions in thickness.

Magnetic analysis, X-ray, optical and transmission electron metallography were all done only on the material within the original 2-inch gage length of tensile specimens where the amount of strain is accurately known. The same specimen was used for the four techniques so that a one-to-one correspondence of results was obtained. Thus, magnetic analysis, X-ray, and optical metallography were done first before preparing specimens for transmission electron microscopy. Observation of the thin foils was done with the Siemens Elmiskop IA operated at 100kV.

Details of the experimental techniques are described fully elsewhere.[16]

III.   EXPERIMENTAL RESULTS

A.   The ε-Martensite:

The X-ray analysis showed the presence of the 10.0, 10.1 and 10.2 reflections typical of unfaulted hcp structures. Thus ε is not randomly faulted fcc, but a perfect hcp phase. Intensity measurements showed that the relative volume fraction of ε reached a maximum amount after about 5% strain and then decreased thereafter, whereas the volume fraction of α increased steadily with increasing amounts of deformation.

The electron diffraction patterns and dark-field microscopy results, illustrated in Figs. 1 and 2, confirm further that the ε-phase is hexagonal. The electron diffraction pattern (Fig. 1a) of the central area in Fig. 1b is schematically drawn and indexed in Fig. 1c. Indexing of Fig. 1a was greatly facilitated by noting the features revealed by the dark-field experiments shown in Figs. 2a, 2b, 2c, 2d, 2e, and 2f, which were due to spots marked A, B, C, D, E, and F, respectively, in Fig. 1c, when these were tilted to the optic axis. A 10μ dia. objective aperture was used to separate the diffraction spots to obtain the images of Fig. 2, which correspond to the central area in Fig. 1b. The dark-field images of Figs. 2a, 2c, and 2d have the same contrast which means that spots A, C, and D (Fig. 1c) came from the same (single) phase. These spots were indexed to be hexagonal and are the (01.0), (01.1), and $(01.\bar{1})$ reflections in the $[2\bar{1}.0]$ zone. The indexed hexagonal pattern revealed the 00.1 double diffraction spot in Fig. 1a, indicated in Fig. 1c. This can only arise from a hcp structure and thus confirms the presence of a hexagonal phase. By the same token, Figs. 2b and 2e, are the images corresponding to the γ-austenite matrix reflections of B and E indexed as $(\bar{1}11)_\gamma$ and $(200)_\gamma$, respectively, in the $[110]_\gamma$ zone.

The last dark-field image, Fig. 2f, reversed contrast in the central

portion (light area) of Fig. 1b. The indexed patterns of the ε and γ show

that the (0002) and (111) spots are coincident in F (Fig. 1c) which explains

the contrast reversals outside the central region. However, the central

region cannot be ε or γ and is actually the α (bcc) phase. The d-value of

$(110)_\alpha$ is very close to the d-values of the (0002) and $(111)_\gamma$ which makes

them overlap at F. In this pattern the orientation of α is very close to

[100].

The ε can be described either as regularly faulted γ, or as an hcp phase

with an ideal c/a ratio. The diffraction pattern, Fig. 1a, shows no shift

in positions of the fcc reflections and the ε reflections occur at all pre-

dicted ideal hcp positions and the (0001) spot appears due to double diffrac-

tion from the hcp structure.[18] Therefore, it is appropriate to define ε

as an hcp phase rather than as faulted austenite. The orientation relation-

ships between γ and ε are simple in that close packed planes and directions

are parallel in both phases. Because of the apparently low stacking fault

energy of the 304 stainless steel, the formation of ε is facilitated by disso-

ciation of dislocations into partials in a manner similar to that observed

in the nucleation and growth of the γ' phase in Al-Ag alloys.[19] The streaks

in Fig. 1a in the $[111]_\gamma$ direction, (sketched in Fig. 1c), indicate that the

ε forms as thin sheets on $\{111\}_\gamma$. These sheets are edge-on, i.e., perpen-

dicular to the plane of the foil, and are seen projected as lines running

bottom left to top right corner (Fig. 1b).

The dark-field images (Fig. 2) illustrate an important point. The

arrow at the central portion of Fig. 1b points to a dark speck which is

reversed in contrast Fig. 2d, and thus must be ε. The central area D in

Fig. 2d and in Fig. 2f was identified as the α-phase. The speck of ε is

within this α particle. This is contrary to one of Otte and Dash's impli-
cations[9] that ε cannot occur within α.

The view that α can form only after ε is further substantiated by the
existence of ε independently of the α as shown by Fig. 3. The ε plates are
seen to have a non-uniform thickness across the entire grain of γ and small
ε flecks occur within the grain and also at grain/twin boundaries. These
observations are consistent with both the Seeger mechanism[20] and Bollmann[21]
theory of fcc→hcp transformations. However, direct observations in Al-Ag
show that heterogeneous nucleation and growth is the most common mode of
transformation.[19]

The ε phase also forms without deformation by isothermal holding below
M_s. This is shown in Fig. 4a where the ε was formed after 72 hours at $-78°C$.
After this treatment, α could not be detected either by X-ray or by magnetic
analysis. Furthermore, ε was also observed after 13% tensile deformation
at room temperature as shown in Fig. 4b. At room temperature, magnetic
measurements[16] revealed the presence of α only after 50% tensile strain.
These facts, together with the result that no α was formed after immersion in
liquid helium for three days indicate the following: 1) the M_d for both the
ε and α phases in this alloy is about 293°K, 2) the M_s for α is less than
4°K, and 3) the M_s for ε must be greater than 195°K. Furthermore since no
ε was observed in the as-quenched samples (to 78°K and 4°K), the trans-
formation of γ to ε and particularly to α is very sluggish, requiring
thermal activation and/or external energy.

B. The Nucleation and Growth of the α Martensite

The α phase was formed only after plastic deformation at temperatures
from room temperature and below. In no case was α observed independently of

ϵ and the nucleation of the α was observed only at 1) intersecting ϵ bands (Figs. 2 and 5), and 2) at or near intersections of ϵ bands with grain or twin boundaries (Fig. 6). On the right part of Fig. 6 is a twin crystal extending from top to bottom. The preferentially nucleated α is indicated at N at the top portion of the twin crystal. At the bottom part of the twin crystal at G are α crystals which seem to have grown as laths across the twin. There is no α between N and G which further confirms that ϵ forms first. In Fig. 6b, the grain boundary runs vertically and the α has formed on the same side where the ϵ bands are.

In Fig. 6a, the area of α between T-T contains debris of dislocations which in region D appears to be inherited from the ϵ (or faulted γ). Remnants of ϵ still remain. Since the particles of α have very irregular shapes, it was not possible to obtain habit-plane determinations.

Figure 7 illustrates that adjacent α crystals do not necessarily have to be twin related as has been observed by others.[9,13] The diffraction pattern (Fig. 7a) of the central area of Fig. 7b is sketched in (c). The indexing of this pattern with the aid of the dark field images shown in Figs. 7d, e, and f revealed only one bcc orientation. The α crystal marked G in Fig. 7b is in the same orientation as the α to its right as illustrated by the dark-field image (7d). This shows that as both nuclei grow, they consume the ϵ which is between them. When the ϵ is pinched at two points with the two α crystals joining as one, e.g., area G in Fig. 6a and Fig. 7e remnants of ϵ can be observed within the α. The α is not internally-twinned but rather heavily dislocated. The dislocations are seen to reverse contrast in Fig. 7d.

C.   Orientation Relationships Between γ, ε, and α.

The Kurdjumov-Sachs (K-S) and the Nishiyama (N) relationships are the well-known orientation relationships between the fcc and bcc phases during the martensitic transformation $\gamma \rightarrow \alpha$ in iron alloys. Theoretically, in both these relationships, the $(111)_\gamma$ is converted into the $(110)_\alpha$ with the $[\bar{1}01]_\gamma$ parallel to the $[11\bar{1}]_\alpha$ in the K-S while the $[211]_\gamma$ is parallel to the $[1\bar{1}0]_\alpha$ in the N relationship. The two orientations are related by a 5°16' rotation of the bcc lattice about the $[110]_\alpha$ axis. Experimentally, however, the observed relationships vary from the theoretical by a few degrees.[1]

However, the results presented here show that the α does not form directly from the γ, but rather from ε. The relationship between γ and ε illustrated in Fig. 1 is simple in that close-packed planes and directions coincide, i.e.,

$$(111)\gamma \,/\!/\, (0001)_\varepsilon \quad \text{and} \quad [10\bar{1}]_\gamma \,/\!/\, [11\bar{2}0]_\varepsilon \; .$$

It has often been reported that the orientation of the terminal phase α to γ is very close to the K-S.[5,7,8,13] In the majority of cases this was also observed in the present work.

However, in several instances, the orientation between the γ and α has been found also to be the N relationship (see e.g. Fig. 1). Figure 8 might indicate how the K-S relationship arises; Figs. 8d, e, f, and g are the dark-field images of spots A, B, C, and D indicated in Fig. 8c. The indexed diffraction pattern revealed that two bcc, one fcc, and one hcp orientation resulted from the region of intersection indicated by the arrow in Fig. 8a of the ε-bands I and II. One bcc pattern has the zone axis $\langle 100 \rangle_\alpha$ indicating the N relationship while the other has the zone axis $\langle 111 \rangle_\alpha$ which corresponds to the K-S relationship. In Fig. 8c, a $\langle 110 \rangle$ direction of one bcc crystal in the $\langle 111 \rangle$ orientation is rotated about 5° from another $\langle 110 \rangle$

direction of the other bcc crystal in the 100 orientation. This is the

predicted angular difference between the N and K-S relationships.

By comparing the dark-field images of Fig. 8d and Fig. 8f which were

from the bcc spots in the $[111_\alpha]$ (K-S) and $[100\ \alpha]$ (N) orientation, respec-

tively, it can be seen that the amount of α in the N orientation is greater

than that in the K-S orientation. Since the K-S is to be the final orienta-

tion between the γ and α , this result may imply that the bcc crystal formed

first in the N orientation.

The sequence of events in Fig. 8a showing two intersecting ε -bands I

and II may be reconstructed as follows. Band I formed first and is the in-

tersected band. It is displaced noticeably in the $[211_\gamma]$ direction (Figs.

8a and 8c) as it is intersected by band II which appears to occur from left

to right, indicating the direction of dislocation motion. At the region

of intersection shown by arrow in Fig. 8a, the α bcc crystal in the N orien-

tation must have formed. On further deformation, dislocations from band II

pile up on the α_1 crystal to build up enough stresses that must somehow

rotate that part of α_1 to the K-S orientation. These observations suggest

a mechanism by which α can be obtained at regions of intersections of two

ε -bands or at regions where an ε -band meets a twin or grain boundary and

will be discussed in Section IIIB.

Another interesting point is also provided by Fig. 8f. The pile-up of

dislocations on α_1 from the left apparently causes it to consume part of

band II to the right. This is suggested by the α_1 crystals pointed by arrows

in Fig. 8f. This observation can explain why the amount of ϵ peaks at fairly

low strains ($\sim 5\%$) and then decreases thereafter. Presumably enough slip

systems are nucleated to provide intersecting regions for the formation of

α crystals. After a certain amount of deformation, the α is able to grow

into pre-existing ε-bands. Further deformation naturally produces more

ε, but the pre-existing ε is consumed at a faster rate which leads to the steady decrease in ε while the α increases proportionately with increasing plastic deformation.

D.   Summary of Experimental Results

The essential findings of this part of the investigation are the following:

1. The formation of α martensite in 304 stainless steel was observed only after plastic deformation. The M_d was estimated to be around 293°K and the M_s <4°K. The amount of α increased with increasing amounts of deformation at 78°K.

2. In this alloy system, the ε is also a thermodynamically stable hcp phase which is formed either by plastic deformation at or below room temperature (M_d) or after isothermally holding at low temperatures, e.g., -78°C for 3 days.

3. The martensitic transformations proceed in the sequence $\gamma \rightarrow \varepsilon \rightarrow \alpha$ and not $\gamma \rightarrow \alpha$ with ε resulting from the large shear deformation. The latter sequence was ruled out on the basis of the new evidence that ε was formed independently of α and also because ε was detected within the α phase.

4. The α phase was preferably nucleated at intersections of two ε bands and at or near regions where the ε band abutts twin or grain boundaries, i.e., at regions under compression.

5. The nuclei of α appear to be needle-like which grow into laths. Growth of the α occurs at the expense of ε which explains why the relative amount of ε decreases after reaching a maximum amount at relatively low strains.

6. Adjacent α crystals within an ε band are not necessarily twin related.

7. The orientation relationship between the γ and α phases appeared to change from the Nishiyama to the Kurdjumov-Sachs during growth.

IV. DISCUSSION OF RESULTS

A. The ε-phase

The occurrence of the hexagonal ε phase besides the γ and α phases is well known in binary Fe-Mn alloys. Schumann[23] showed convincingly that the α nucleated within the ε phase and not in the γ. The size of the α is limited by the ε and the thickening of α crystals within the ε lead to the description of lath-martensite.[13] In the range of 10-14.5%Mn, the ε and α co-exist in the structures and separate M_s temperatures of the γ → ε $(M_s)^\epsilon$ and ε → α $(M_s)^{\epsilon \to \alpha}$ transformations were detected.[23] For the 13.83%Mn alloy, the M_s^ϵ is 160°C and the $M_s^{\epsilon \to \alpha}$ is 140°C. This substantiated the metallographic evidence that ε is a phase from which α can be nucleated.

The results of the present investigation show also that in Fe-Cr-Ni stainless steels, α is nucleated from ε. This question has not been unambiguously resolved until now.

In the sequence of transformation γ → ε → α in stainless steels, there is the possibility for two distinct M_s temperatures to exist, as has been observed in Fe-Mn alloys.[23] Goldman, Robertson and Koss[14] used three techniques, viz., differential thermal analysis, temperature dependence of resonant frequency (elastic moduli) and internal friction, to follow the transformations in an Fe-15.1Cr-11.7Ni alloy in the hope of detecting a separate M_s^ϵ above the M_s^α (γ → α). Since this was not observed, it was concluded that the transformation sequence was that proposed by Dash and Otte.[9] However, Schumann[23] pointed out the difficulty of using thermal analysis to record two separate M_s temperatures even in the Fe-Mn alloys. In the range 10-14.5% Mn, the steels with 11.18% and 12.75% Mn yielded only a single M_s point. In these alloys, the predominant phase is α which forms

from ε. Two separate M_s points were found only in the 13.83% Mn alloy

mentioned above. Another difficulty that might arise in using thermal

analysis is that associated with the low free energy change ($\sim$50 cal/mole)

in the martensitic fcc→hcp transformation.[22] All the arguments about

the correct sequence of reactions in the Fe-Cr-Ni alloy systems is quite

unfortunate in that the results are drawn from widely different compositions.

Since ε is a stable phase, the transformation ε → α implies an equilibrium

transformation line between these two phases as is now well-known in pure

iron[25] and Fe-Mn alloys.[23] The experimentally determined P-T phase

diagram for pure iron due to Bundy[25] shows that the transformation line

between ε → α in pure iron is similar to that in Fe-Mn alloys.[23,28] A

comparison of the characteristics of the ε phases in pure iron and Fe-Mn

alloys revealed that they are identical.[29] Thus, it appears that the

formation of the ε phase in pure iron can be accomplished either by high

hydrostatic pressures or by suitable alloying additions.[33] Other alloy

systems that show the existence of the ε phase are the Fe-Ru[30] and Fe-Ir[31]

systems. These systems including the Fe-Cr-Ni alloys where ε was observed

are characterized by a common average group number (AGN), i.e., average

outer shell electron concentration, of 7.7-8.2[28] where the occurrence of

the ε phase has been predicted.[32] Another possibility of course is for

alloying to lower the stacking fault energy of γ sufficiently to favor forma-

tion of ε. The ε → α transformation line in Fe-Cr-Ni alloys, as well as

the Fe-Ru and Fe-Ir systems, has yet to be determined. The existence of

a similar transformation diagram in the Fe-Cr-Ni alloys as in Fe-Mn will

illustrate the effect of composition on the formation of different phases.[29]

Thus, at the triple point, it is expected that both ε and α are formed

simultaneously, while below the triple point composition, the γ → α trans-

formation is expected.

It is, however, a fact that in pure iron[25] and Fe-Mn alloys[29] although the $\varepsilon \to \alpha$ will proceed, the reverse $\alpha \to \varepsilon$ cannot be effected. In pure iron,[25] it is necessary to revert the α to γ in order to allow ε to form from the γ on cooling at a constant hydrostatic pressure. The $\varepsilon \to \alpha$ reaction in pure iron means that a lower symmetry hcp structure is transformed to a higher symmetry cubic structure. This result is contrary to one of the arguments used by Dash and Otte[9] against the $\gamma \to \varepsilon \to \alpha$ sequence of reactions in the Fe-Cr-Ni alloys. It needs to be mentioned only that the $\varepsilon \to \alpha$ reaction occurs in both pure Fe and Fe-Mn alloys and the similarity of these systems with Fe-Cr-Ni alloys lends support to the sequence $\gamma \to \varepsilon \to \alpha$ as a general reaction depending on composition (stacking fault energy) and thermodynamic variables (particularly pressure).

B.   The Nucleation of α From ε

It has been observed that the nucleation of α preferentially occurs at intersections of two ε-bands or where the ε-band meets either a grain boundary or twin boundary. If one considers the expansion of the ε phase in the γ matrix to occur by motion of $a/6 \langle 211 \rangle_\gamma$ dislocations as is expected for fcc$\to$hcp transformation,[19] the pile-up of such dislocations against twin or grain boundaries produces a compressed region near the boundaries. Such a compressed region also exist at intersections of two stacking faults as shown by Ashbee.[24] Thus, the nucleation of α by ε is characterized by the presence of a compressive region and the compression is unilateral in the $\langle 211 \rangle_\gamma$ direction.

Since ε is a denser phase than α, it is expected that ε is more stable at higher pressures. It seems, therefore, that at the compressed regions

cited above that the ε would be rendered more stable. This is certainly

true if the compression is multilateral, i.e., hydrostatic.[25] However,

in a unilateral or at most bilateral compression, as will be seen later,

and because of the tendency to form α, the compression will bring the ε

to a higher energy state than its surroundings. The excess pressure at

the compressed regions of ε can be relieved if an expansion to the bcc

lattice occurs, since for the same force a larger volume will experience

a smaller pressure. Such an expansion is possible because of the absence

of hydrostatic pressure. Bundy's work[25] corroborates this explanation

in that the lower pressure phase in iron is α. These arguments also suggest

that if formation of α through this process is achieved at lower tempera-

tures, raising the temperature to relieve the pressure would tend to pro-

duce more α. This has been observed[16] and will be considered in another

paper.[17]

As soon as α nucleated, its growth can be considered in the following

manner. The volume expansion on transformation to α will necessary put

pressure on the surrounding phases and again to relieve this pressure, the

α will form. A repetition of this process creates a natural "Umklapp" pro-

cess which is characteristic of martensitic transformations.

The observations that a compressive stress is present in the $\langle 211 \rangle_\alpha$

and also that the Nishiyama orientation relation was observed at the start

of the transformation suggest the atom movements shown in Fig. 9. In this

figure, the hcp structure is shown with the atoms in the (0001) as filled

circles and the atoms in the (0002) plane as open-circles. When the atoms

in the open-circled positions are moved the distance $\left| \frac{\vec{a\gamma}}{12} \langle 211 \rangle \right|$ (equivalent

notations in fcc are used for simplicity) to the center of the prismatic

planes in the cross-circled positions, an essentially bcc structure in the

Nishiyama orientation is obtained except for certain angular and dimensional

changes. This movement is seen to be the direction of motion of partial

dislocations in the $\{111\}_\gamma$ and is equivalent to the system $\{110\} \langle 1\bar{1}0 \rangle_\gamma$ in

the bcc structure. Zener[27] showed that in the bcc structure the motion

of atoms along this direction offers negligible resistance if the atoms are

packed as hard spheres.

An outline of a $(110)_\alpha \| (111)_\gamma$ is also indicated in Fig. 9. In order

to obtain the actual bcc structure, it is necessary to deform the hcp

structure along the principal directions $\langle 211 \rangle_\gamma$ and $\langle 110 \rangle_\gamma$ in the $\{111\}_\gamma$

and along the $\langle 111 \rangle_\gamma$ $(0001)_\varepsilon$. The resulting principal distortions are

-0.0819, +0.126, and -0.0242, respectively (see Fig. 10). These deforma-

tions can be achieved if a biaxial compressive stress system along the $\langle 211 \rangle_\gamma$

and $\langle 111 \rangle_\gamma$ directions can be applied to the hcp structure as shown in Fig.

10a. This suggests that an added $\langle 111 \rangle_\gamma$ compressive stress is needed on

top of the $\langle 211 \rangle_\gamma$ compressive stress. One notes, however, that the com-

pressive strain in the $\langle 211 \rangle_\gamma$ is more than three times that in the $\langle 111 \rangle_\gamma$

and perhaps the latter could be achieved with only the $\langle 211 \rangle_\gamma$ compressive

stress. This might be plausible since the (c/a) ratio in ε is ideal. In

this situation, the atoms can be considered packed as hard spheres and the

bonding of atoms is principally due to nearest neighbor interactions along

their interatomic distance (central force approximation).

The principal lattice distortions in transforming the hcp structure

to the bcc is defined only by the positions of the corner atoms of the hcp

unit cell. The slight rearrangement or internal shuffling of the atom at

1/3, 2/3, 1/2 does not contribute to the lattice deformation. Pitsch[26]

pointed out that these geometric conditions must be met in a transformation

process with cooperative movements of atoms , i.e., in the martensitic trans-

formation.

V.   SUMMARY

It has been proved that the sequence of martensitic transformations
in 304 stainless steels is $\gamma \to \epsilon \to \alpha$.   This conclusion is based mainly on
newly acquired evidence that 1) the ϵ can exist inside the α phase; and
2) ϵ formed independently and before the formation of α, i.e., α was never
found unless associated with ϵ. ϵ is a thermodynamically stable hcp phase.
Comparison of the above sequence with the $\epsilon \to \alpha$ reactions in pure iron and
in iron-manganese alloys suggests that a similar equilibrium transformation
line between ϵ and α known for these systems might be found in Fe-Cr-Ni
alloys.   Nucleation of the α was observed principally at intersections of
two ϵ-bands or an ϵ-band with twin or grain boundaries which represented
unilaterally compressed regions.   Electron diffraction indicates that the
Nishiyama relationship between γ and α phases is predominant at the start
of the transformation which later changed to the Kurdjumov-Sachs.   Based
on these experimental findings, a sequence of atom movements from the hcp
to the bcc structure was proposed having the basic geometric conditions of
a martensitic transformation.

UCRL-18868

ACKNOWLEDGEMENT

REFERENCES

1. C. M. Wayman, "The Crystallography of Martensitic Transformations in Alloys of Iron", (In press).

2. B. Cina, Acta Met., 1958, 6, 748.

3. B. Cina, J. Iron Steel Inst., 1954, 177, 406.

4. R. P. Reed, Acta Met., 1962, 10, 865.

5. J. F. Breedis and W. D. Robertson, Acta Met., 1962, 10, 1077.

6. R. P. Reed and C. J. Guntner, Trans. Met. Soc. AIME, 1964, 230, 1713.

7. R. Lagneborg, Acta Met., 1964, 12 823.

8. J. A. Venables, Phil. Mag., 1962, 7, 35.

9. J. Dash and H. M. Otte, Acta Met., 1963, 11, 1169.

10. H. M. Otte and J. Dash, Electron Microscopy, Vol. A, (1964). Proceedings of the Third European Regional Conference, Prague, 1964.

11. J. F. Breedis, Trans. Met. Soc. AIME, 1964, 230, 1583.

12. P. M. Kelly and J. Nutting, J. Iron Steel Inst., 1961, 197, 199.

13. P. M. Kelly, Acta Met., 1965, 13 635.

14. A. J. Goldman, W. D. Robertson, and D. A. Koss, Trans. Met. Soc. AIME, 1964, 230, 240.

15. C. J. Guntner and R. P. Reed, Trans. ASM, 1962, 55, 399.

16. P. L. Mangonon, Jr., UCRL Report 18230, Lawrence Radiation Laboratory, University of California, Berkeley, California.

17. P. L. Mangonon, Jr., and G. Thomas, UCRL-18869, LRL, Berkeley, Calif.

18. G. Thomas, W. Bell, and H. M. Otte, Phys. Stat. Sol., 1965, 12, 353.

19. J. A. Hren and G. Thomas, Trans. AIME, 1963, 227, 308.

20. A. Seeger, Z. Metallkunde, 1956, 47, 653; 1953, 44, 247.

21. W. Bollman, Acta Met., 1961, $\underline{9}$, 972.

22. L. Kaufmann, "Physical Properties of Martensite and Bainite," I. S. I.
     Special Report 93, (London, 1965) 48.

23. H. Schumann, Arch. Eisenh., 1967, $\underline{38}$, 647.

24. K. H. G. Ashbee, Acta Met., 1967, $\underline{15}$, 1129.

25. F. P. Bundy, J. App. Phys., 1965, $\underline{36}$, 616.

26. W. Pitsch, Arch. Eisenh., 1967, $\underline{38}$, 853.

27. C. Zener, "Elasticity and Anelasticity of Metals", University of
     Chicago Press, 1948.

28. H. Schumann, Z. Metallkunde, 1967, $\underline{58}$, 207.

29. H. Schumann, Neue Huette, 1966, $\underline{11}$, 299.

30. L. D. Blackburn, L. Kaufmann, and M. Cohen, Acta Met., 1965, $\underline{13}$, 533.

31. M. Miyagi and C. M. Wayman, Trans. Met. Soc. AIME, 1966, $\underline{236}$, 806.

32. W. Hume-Rothery, Acta Met., 1966, $\underline{14}$ 560.

33. J. Genschaft, Phys. Metals Metallography, 1964, $\underline{18}$, No. 1, 107.

FIGURE CAPTIONS

Fig. 1 - Identification of phases in a partially transformed sample. Deformed 15% in tension at -196°C, (a) Diffraction pattern of central area of bright-field image in (b), (c) Indexed pattern -- the pattern consists of three superimposed reciprocal lattice sections of the γ(fcc), α(bcc), and ϵ(hcp) phases.

Fig. 2 - Dark-field images due to spots A, B, C, D, E, and F shown in Fig. 1c. The circle defines the image of the 20μ selected area aperture.

Fi.g 3 - Formation of the ϵ-phase after 4% deformation at -196°C; (a) Diffraction pattern of area shown in b, c, d; (b) Bright field; (c) and (d) Dark-field images of γ and ϵ phase, respectively, showing there is no α present.

Fig. 4 - Dark-field images of the ϵ-phase; (a) Sample held for 3 days at -78°C; (b) Sample tensile strained 13% at room temperature.

Fig. 5 - Nucleation of needle-shaped α particles at intersections (arrow) of ϵ-bands. Specimen deformed 15% in tension at -196°C.

Fig. 6 - Nucleation of α where ϵ-band meets, (a) twin, or (b) grain boundaries. Specimens deformed 15% in tension at -196°C.

Fig. 7 - Showing that adjacent α crystals are not necessarily twin related; (a) Diffraction pattern of (b) Bright field; (c) Indexed pattern; (d), (e), (f) Dark-field images of spots A, B, and C in (c); (d) shows that the adjacent crystals are not twin related. Specimens deformed 15% in tension at -196°C.

Fig. 8 - Orientation of γ and α is apparently NIshiyama (N) at start of transformation which changes to the Kurdjumov-Sachs (K-S).

Fig. 8 - (a) Bright field; (b) Diffraction pattern; (c) Indexed pattern;
(Contd)
           (d), (e), (f), (g) Dark-field images of spots A, B. C, and D in (c).

           Specimens deformed 4% at -196°C.

Fig. 9 - Suggested probable atom movements in the hcp to bcc transformation.

Fig. 10- Dimensional and angular changes in the hcp to bcc transformation
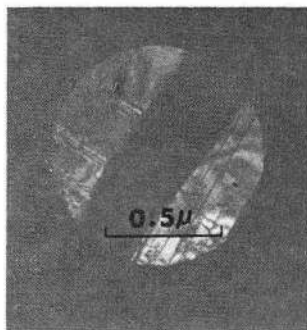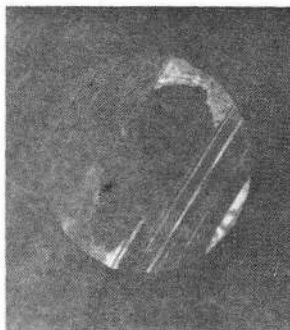
           suggested by Fig. 9.

Fig. 1

0.5μ
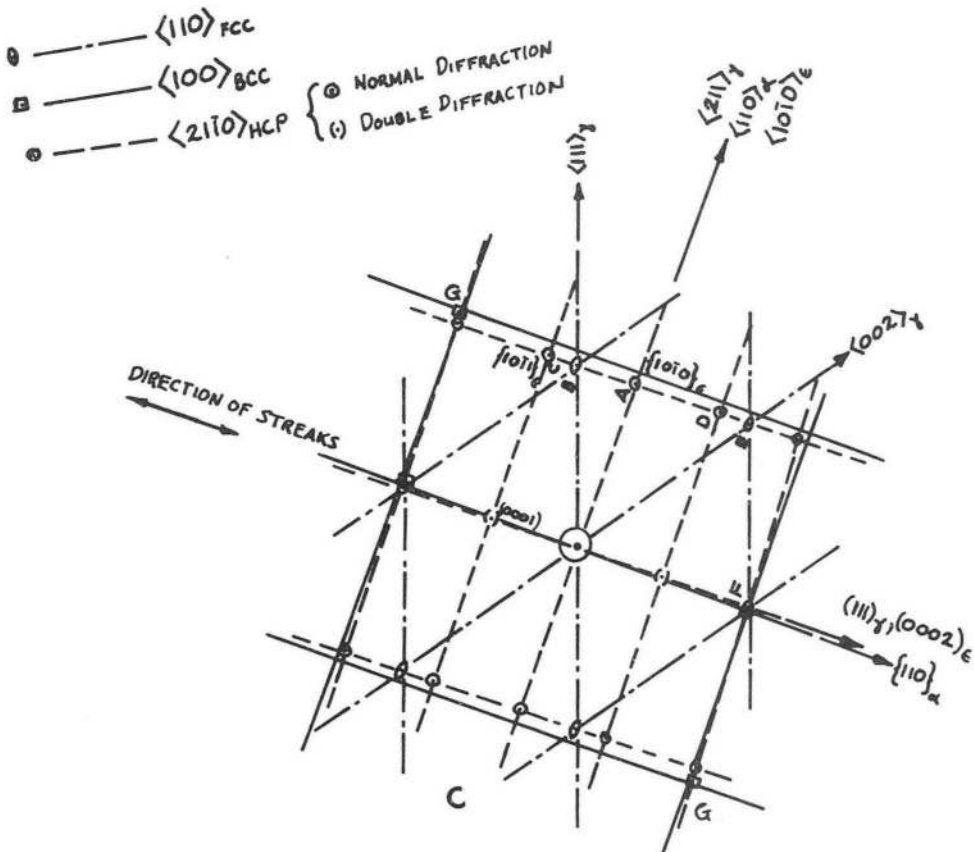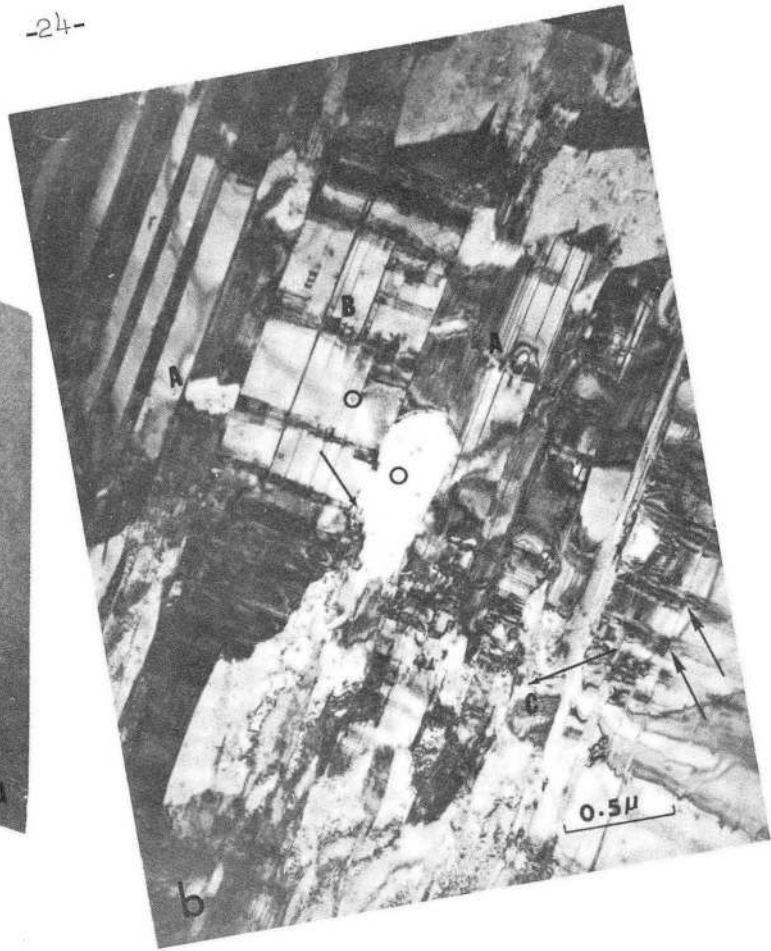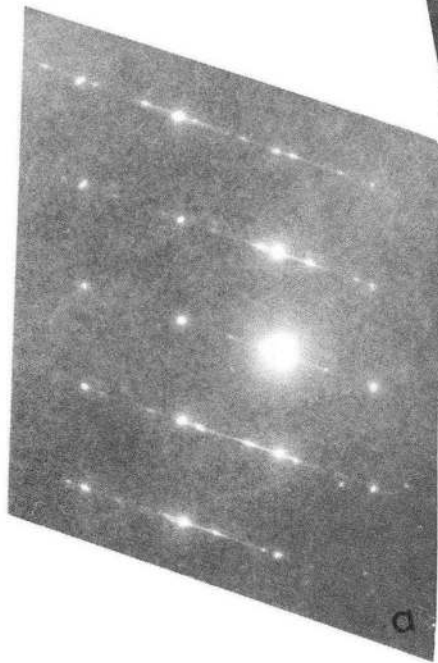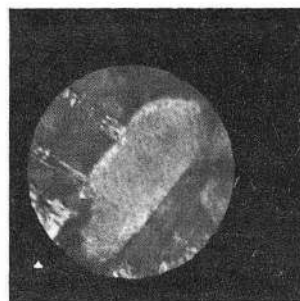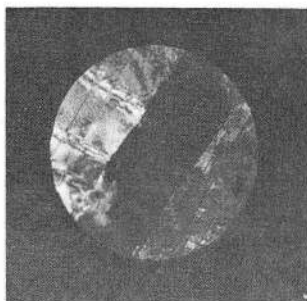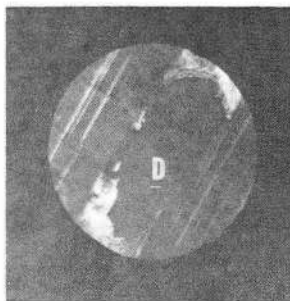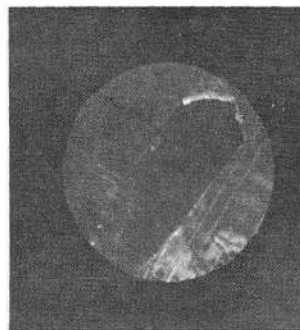
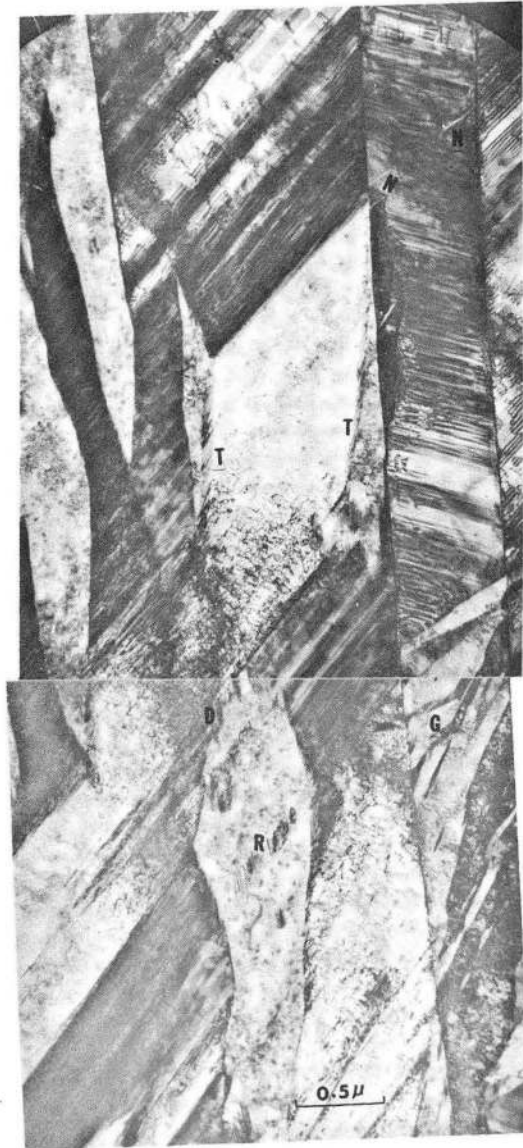XBB 685-2533

Fig. 2
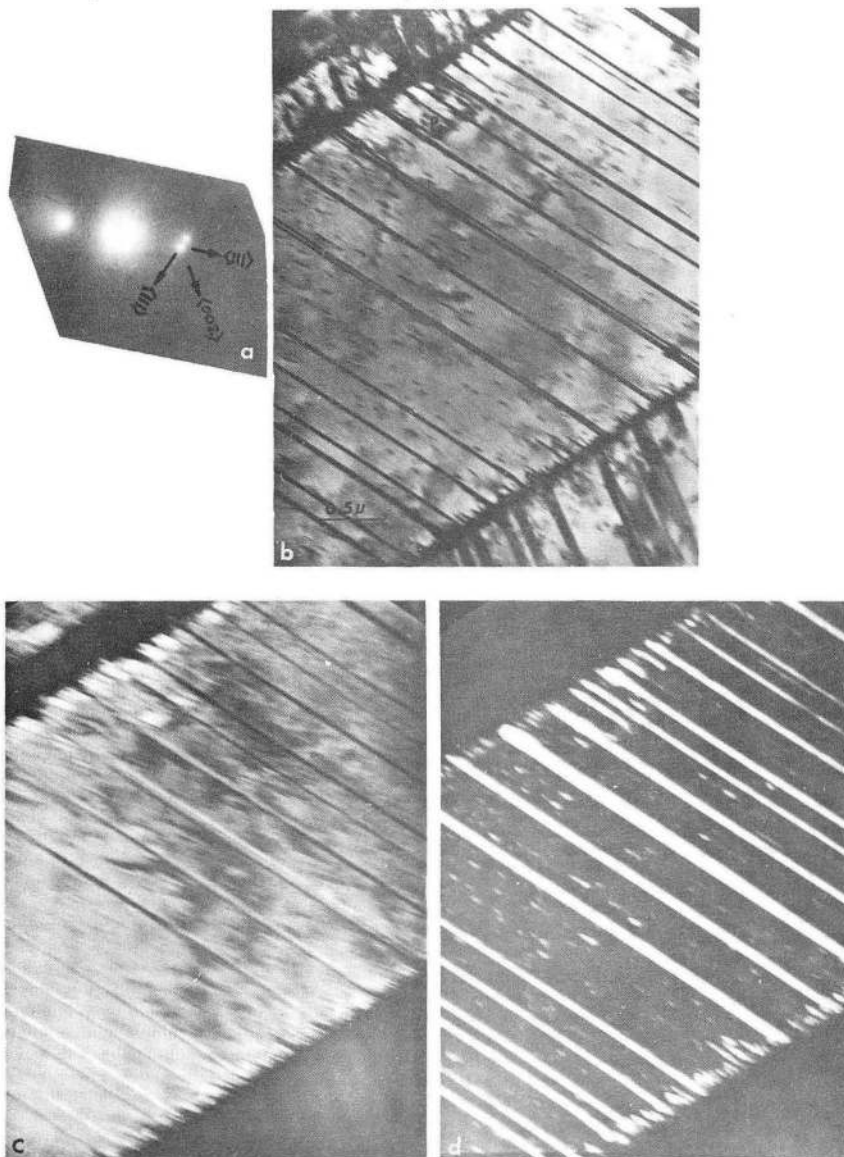
XBB 685-2525A

Fig. 3
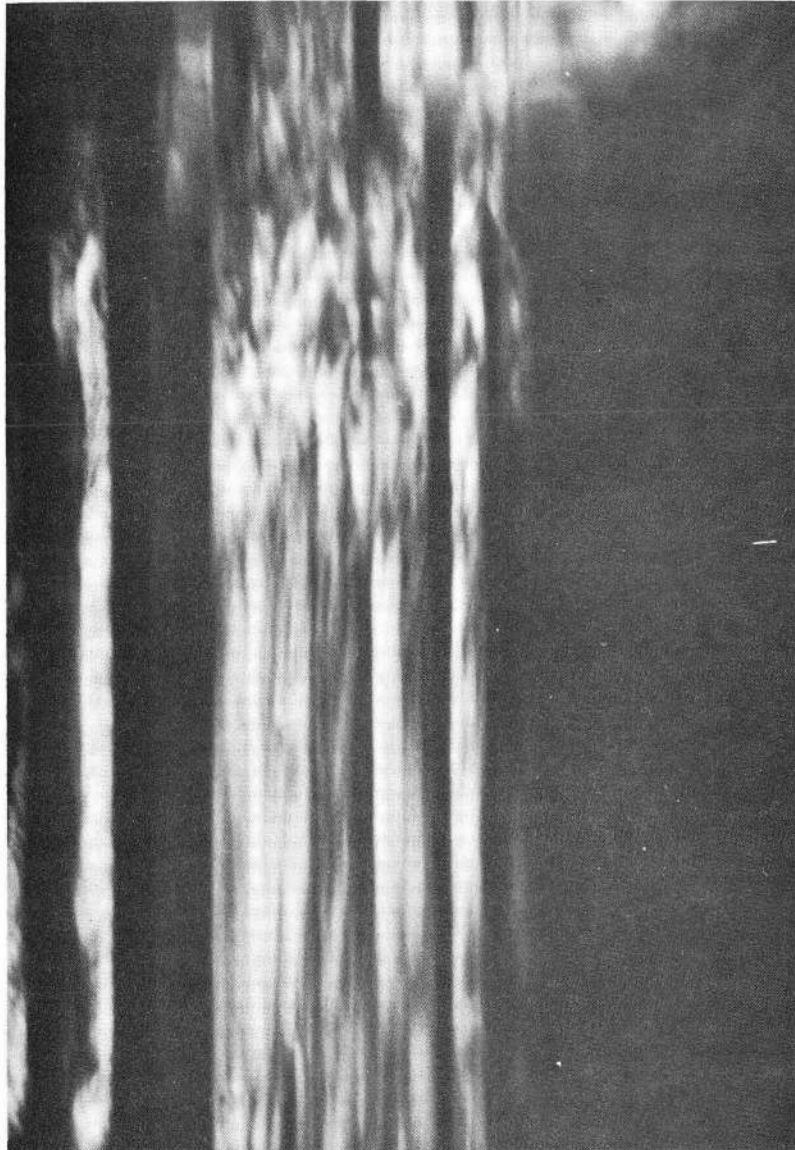
XBB 687-4097A

Fig. 4 (a)

XBB 685-2532A

Fig. 4 (b)

0.5μ

XBB 687-4083

Fig. 5

XBB 685-2524

Fig. 6 (a)

0.5μ

XBB 687-4098

Fig. 6(b)

Fig. 7

Fig. 8

XBB 685-2537A

XBB 685-2531A

Fig. 8

$$\frac{c}{a} = 1.63$$

XBL 687-1290

Fig. 9

$\sigma_{[0001]_\epsilon} = \sigma_{[111]_\gamma}$

$[0001] = [111]_\gamma$

$[\bar{1}\bar{1}20]$

$\sigma_{[1100]_\epsilon} = \sigma_{[\bar{2}11]_\gamma}$

$C = 4.14 \text{Å}$

0.733Å

$120°$

VOLUME / 2 ATOMS = 23.10Å^3

(a)

$[\bar{1}100] = [\bar{2}11]_\gamma$

$60°$

$\vec{a} = 2.54 \text{Å}$

$[11\bar{2}0]_\epsilon = [01\bar{1}]_\gamma$

$60°$

$2.54 \times 2 \times \sin 60° = 4.40 \text{Å}$

$70.5°$

(b)

XBL 687-1291

Fig. 10